High Spatial and Temporal Resolution Cardiac Imaging Reconstructed from Real-Time Golden Angle Radial Acquisitions using Motion Correction and Parallel Imaging

M. S. Hansen[1], T. S. Sørensen[2], and P. Kellman[1]

[1]National Heart, Lung, and Blood Institute, National Institutes of Health, Bethesda, MD, United States, [2]Department of Computer Science, Aarhus University, Aarhus, Denmark

Introduction

Real-time cardiac MRI is a valuable alternative to traditional breath-held cardiac gated cine imaging in patients with arrhythmias or difficulty breath holding. Unfortunately, the real-time images are often inferior in diagnostic quality to breath-held, gated acquisitions. For Cartesian acquisitions, it has been demonstrated that registered real-time images from multiple RR intervals can either be averaged to improve SNR (1) or the k-space data from the registered images can be recombined to yield images with higher temporal resolution and improved SNR (2). In this work we introduce the non-trivial extension of this principle to arbitrary trajectories and we demonstrate retrospective reconstruction of high spatial and temporal resolution cardiac image series based on real-time acquisitions using the radial Golden Angle acquisition scheme (3). This acquisition scheme allows reconstruction of images with arbitrarily wide temporal window at an arbitrary point in time, i.e. it is possible to reconstruct low temporal resolution images centered corresponding to the acquisition of any of the acquired data profiles and use these low temporal resolution images to determine the deformation due to respiratory motion at the time the data was acquired. The proposed reconstruction algorithm includes this deformation into the encoding description (4) and uses a conjugate gradient solver to reconstruct the images.

Materials and Methods

Data was acquired in five (N=5) healthy volunteers (with written informed consent and IRB approved study protocol) using an SSFP radial sequence (TE=1.52ms, TR=3.04, α=50°, FOV=350-400, matrix=256x256) modified to use a golden angle profile-ordering scheme (3). A slice was prescribed in a mid-ventricular short axis orientation and real-time data was acquired over a period of 30 seconds. Each individual k-space profile was assigned a time in the cardiac cycle based on an ECG signal and in a retrospective processing step the cardiac cycle timing was normalized for all acquired profiles to compensate for any RR interval variation during the acquisition. Thirty cardiac phases were reconstructed using the following reconstruction algorithm (see Fig. 1). For each covered RR interval, a wide temporal window was used to select 100 radial profiles centered on the time for a given cardiac phase and this data was used to reconstruct (using non-Cartesian SENSE) a low temporal resolution image for each RR interval. The low temporal resolution images were registered (optical flow, Horn-Schunck) to a reference respiratory state (end expiration) such that a deformation field corresponding to each RR interval was obtained. A narrow data selection window (~30ms or 10 profiles) was used to select the data from each RR interval that was included in the reconstruction of a specific cardiac phase. The high temporal resolution reconstruction with respiratory motion correction for each cardiac phase was found using the equation $(\mathbf{E}^H\mathbf{E} + \lambda^2\mathbf{L}^H\mathbf{L})\rho = \mathbf{E}^H m$, where ρ is the reconstructed image, m is the measured data, and $\mathbf{E}$ is the encoding matrix consisting of a) Deformation, b) Multiplication with coil sensitivities (S), c) Fourier transform to k-space, and d) sampling on the golden angle radial trajectory. The matrix $\mathbf{E}^H$ consists of a) interpolation of data onto Cartesian grid, b) inverse Fourier transform, c) multiplication with complex conjugate of coils sensitivity map (S^*), and d) the transpose of the deformation. The last step was achieved by forming a sparse matrix describing the deformation (and associated interpolation) and transposing that matrix. The matrix $\mathbf{L}$ was a diagonal regularization matrix constructed with the reciprocal of the expected signal intensity obtained from a time average reconstructed from all the available data. The regularization factor λ was set to 0.5 in all reconstructions.

Results

The motion corrected reconstruction was successful in all five volunteer datasets and Fig. 2 shows example results from one volunteer. From left to right is seen a) reconstruction obtained by simply gridding all available data, b) reconstruction with all available data and parallel imaging (without respiratory motion correction), and c) the full respiratory motion corrected reconstruction. The x-t plots from a profile indicated by the white line are seen below each reconstruction. Notice the marked improvement in image sharpness and motion fidelity in the motion correction reconstruction.

Discussion

The matrix formulation of motion correction (4) provides a powerful framework for removing motion artifacts and blurring. Here we have demonstrated that the golden angle profile ordering scheme can provide low temporal resolution images that can be used to determine the deformation due to respiration and that this deformation information can be used to obtain high spatial and temporal resolution reconstructions from real-time data acquired during free breathing. Conceptually, this is generalization of a method for retrospective motion correction of Cartesian real-time imaging (2), but this extension is not straightforward due to the non-Cartesian sampling. The presented method includes the deformation into the encoding formulation and thus provides a general way of obtaining retrospective gated, high-resolution cine images from arbitrary sampling schemes. Furthermore, since parallel imaging is included in the final reconstruction step, the method is more robust to undersampled regions in k-space.
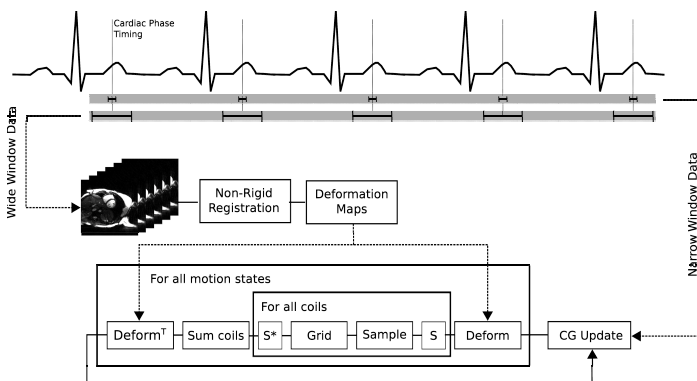

Figure 1. Reconstruction algorithm outline. A wide temporal is used to reconstruct images for non-rigid registration. Data from a much narrower window is then used in the conjugate gradient (CG) reconstruction.
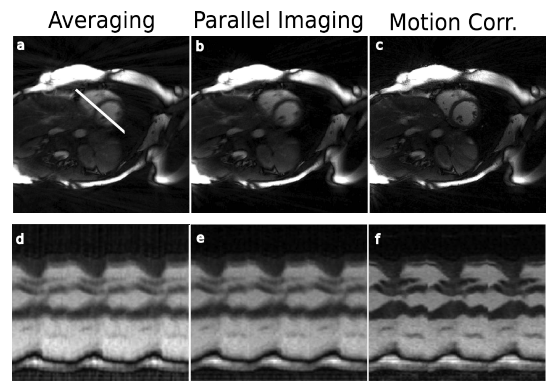

Figure 2. Results from a volunteer. a+d) reconstruction by gridding all data, b+e) All data and parallel imaging in reconstruction, c+f) using both parallel imaging and motion correction as indicated in Fig. 1.

References

1) Kellman et al. Magn Reson Med. 2008 April;59(4):771-8. 2) Kellman et al. Magn Res Med. 2009; 62:1557–1564. 3) Winkelmann et al. IEEE Trans Med Imaging. 2007 Jan;26(1):68-76. 4) Batchelor et al. Magn Reson Med. 2005 Nov;54(5):1273-80.